

Electronic supplementary information

Amorphous carbon supported MoS₂ nanosheets as effective catalyst for electrocatalytic hydrogen evolution

Xue Zhao ^{a,b} Hui Zhu^a and Xiurong Yang^{*a}

^a State Key Laboratory of Electroanalytical Chemistry, Changchun Institute of Applied Chemistry, Chinese Academy of Sciences, Changchun 130022, Jilin, China. E-mail: xryang@ciac.ac.cn

^b University of the Chinese Academy of Sciences, Beijing 100049, China.

1 Experimental details

1.1 Chemicals

$\text{Na}_2\text{MoO}_4 \cdot 2\text{H}_2\text{O}$ and MoS_2 were purchased from Sigma-Aldrich (America), NH_2CSNH_2 was purchased from Sangon Biotech (Shanghai, China), and $\text{C}_6\text{H}_{12}\text{O}_6$ was purchased from Sinopharm Chemical Reagent Co.,Ltd (Shanghai, China). Pt (20% on carbon black) was purchased from Alfa Aesar. All aqueous solutions were prepared with water from a Milli-Q Pore water system (18.2 M Ω).

1.2 IR-compensation

IR-compensation was determined directly on the CHI660B before each Linear Sweep Voltammetry. According to the measurement by CHI660B, the corrected series resistance value was about 6 ohm for the as-prepared MoS_2/AC , while the control samples had corrected series resistance values higher than 6 ohm. This result is in accordance with the EIS measurement.

1.3 Experimental phenomenology

During the HER process, H_2 bubbles were drastically generated from working electrode. There were also bubbles generated and released from the anode obviously, which were identified as oxygen, corresponding to the other half cell reaction of water splitting. $\text{OH}^- \rightarrow 0.5 \text{O}_2 + \text{H}^+ + 2\text{e}^-$.

1.4 Calibrate to reversible hydrogen electrode (RHE)

In all measurements, we used Ag/AgCl electrode as the reference electrode. It was calibrated with respect to reversible hydrogen electrode (RHE). The calibration was performed in the high purity H_2 saturated electrolyte with a Pt wire as the working electrode. CVs were run at a scan rate of 1 $\text{mV} \cdot \text{s}^{-1}$, and the average of the two potentials at which the current crossed zero was taken to be the thermodynamic potential for the hydrogen electrode reactions. In 0.5 M H_2SO_4 , $E(\text{RHE}) = E(\text{Ag}/\text{AgCl}) + 0.204 \text{ V}$. All the potentials reported in this manuscript were against RHE.

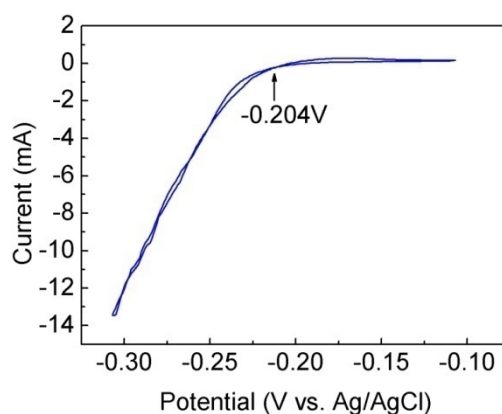


Fig. S1 Calibration of the reference electrode against the RHE.

2 Additional data and discussions

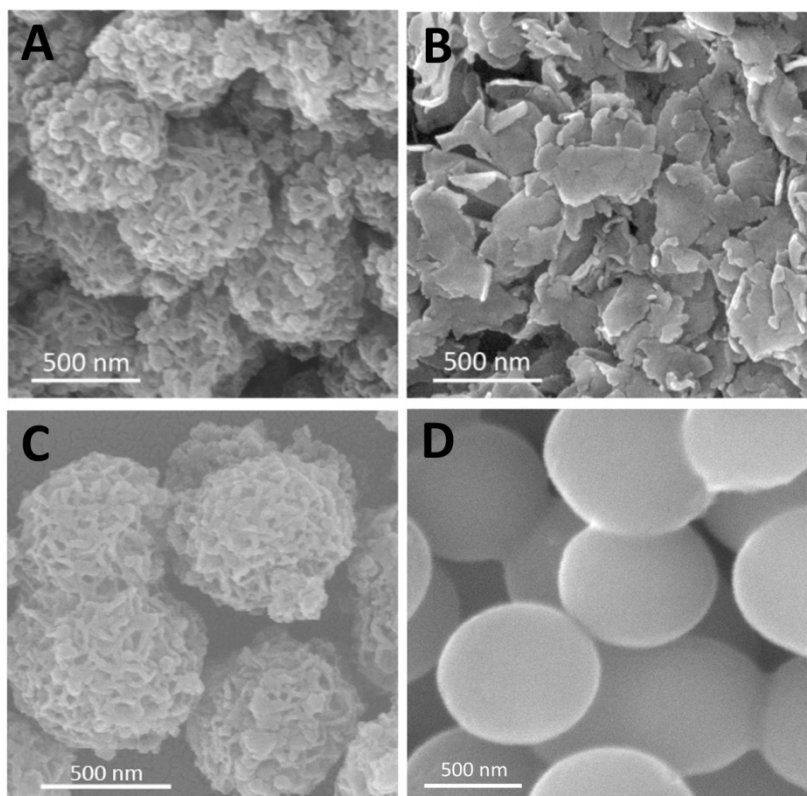


Fig. S2 SEM images of (A) fresh prepared MoS₂/AC, (B) pure MoS₂ nanoparticles, (C) the catalyst ink stored for half a year, (D) MoS₂-free AC.

As shown in Fig. S 2A and 2C, the SEM image of MoS₂/AC stored for half a year was identical to that of fresh prepared. Control experiments were also conducted either in the absence of carbon or MoS₂ by following the exactly same procedure, which resulted in the aggregation of MoS₂ particles (Fig. S 2B) and carbon nanoparticles (Fig. S 2D), both revealing low activities.

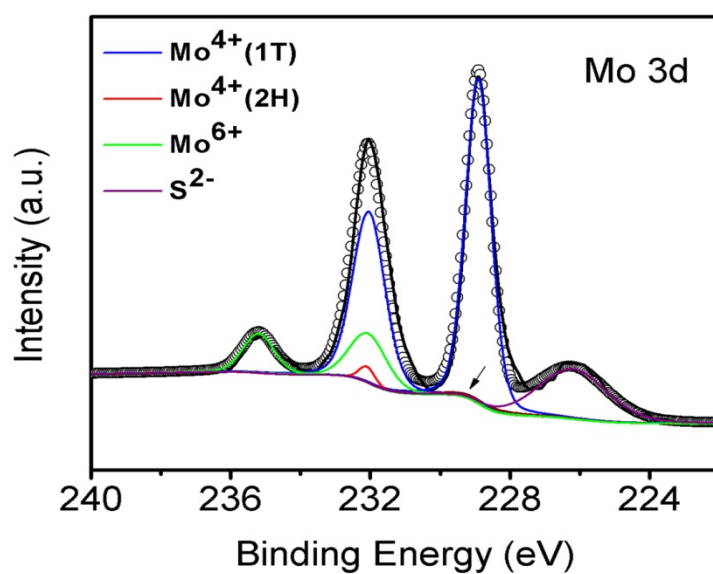


Fig. S3 The deconvolution of Mo3d XPS spectrum of the MoS₂/AC.

The deconvolution of the Mo3d bands indicates the co-existence of the 2H and 1T phases, and the dominant existence of the 1T phase is obvious. It's important to note that the peak intensity of 2H is low, with the peak at about 228.9eV for 2H phase covered by other curves. The 2H and 1T structures are different in the stacking order of S-Mo-S sandwiched tri-layer, indicating that the stacking order of S-Mo-S in the 2H structure is a-B-a and that in the 1T structure is a-B-c.^{1,2}

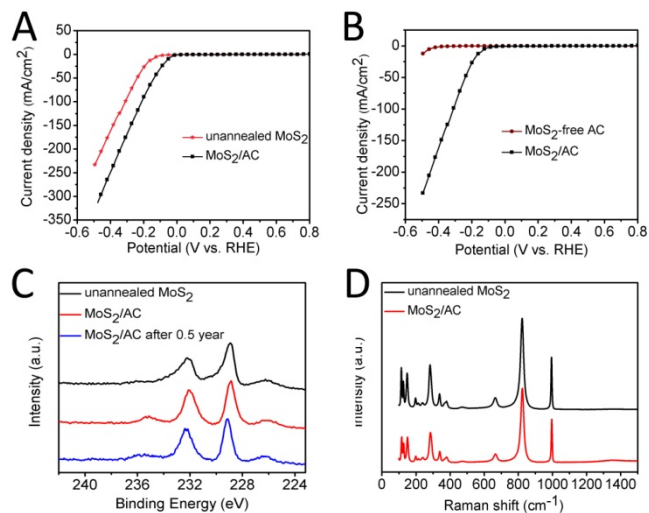


Fig. S4 (A) Polarization performance curves of MoS₂/AC and unannealed MoS₂. (B) Polarization performance curves of MoS₂/AC and MoS₂-free AC. (C) XPS of unannealed MoS₂, as-prepared MoS₂ and MoS₂/AC after 0.5 year. (D) Raman spectroscopy of unannealed MoS₂ and MoS₂/AC.

Table S1 HER parameters of various MoS₂ samples.

Materials	Tafel slope [mV decade ⁻¹]	Tafel region [mV]	j_0 [mA cm ⁻²]	j [mA cm ⁻¹]
Pt	30	10-70	3.39	207
MoS ₂ /AC	40	20-80	4.74×10 ⁻¹	91.4
unannealed MoS ₂	103	100-200	8.71×10 ⁻²	14.7
commercial MoS ₂	107	130-200	1.58×10 ⁻²	1.19
pure MoS ₂	160	250-400	2.10×10 ⁻²	5.22×10 ⁻¹

All the parameters were measured under the same conditions. The values of “ j ” are calculated at overpotential = 200 mV.

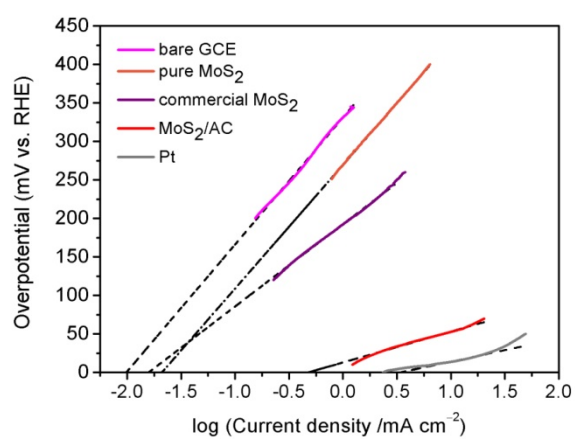


Fig. S5 Calculated exchange current densities of various samples by applying extrapolation methods.

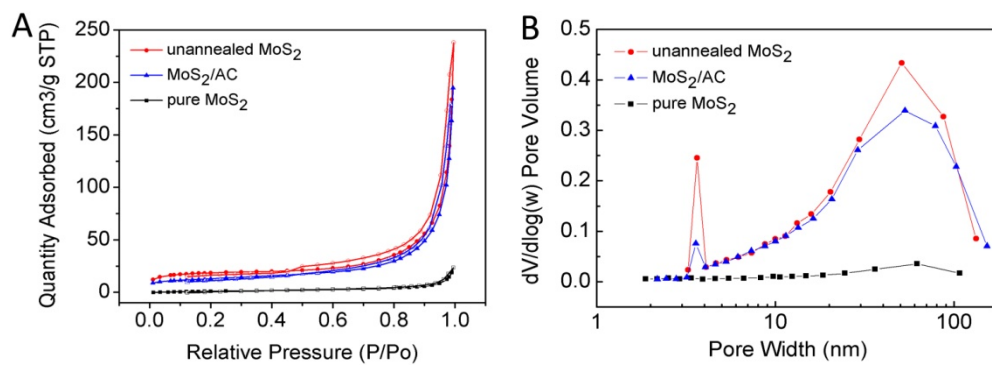
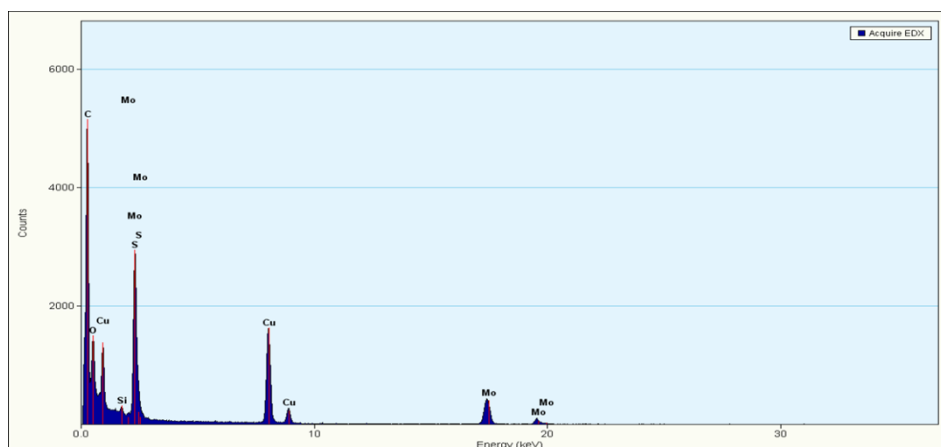


Fig. S6 Nitrogen adsorption-desorption isotherms (A) and the corresponding BJH Desorption $dV/d\log(w)$ Pore Volume plot (B) for various MoS₂ samples: unannealed MoS₂ (red), MoS₂/AC (blue) and pure MoS₂ (black).

Table S2 BET surface areas and catalytic activities toward HER for various samples.

Sample	Tafel slope [mV/dec]	S_{BET} [m ² /g]	j_0 [mA/cm ²]	Normalized j_0 [mA/cm ² _{BET}]
commercial MoS ₂	107	28.0	0.165	2.08×10^{-3}
unannealed MoS ₂	103	58.8	8.71×10^{-2}	5.23×10^{-4}
MoS ₂ /AC	40	43.9	4.74×10^{-1}	3.82×10^{-3}

Herein, quantitative analysis of BET data shows the relationship between the specific surface and catalysis activity. Generally, larger BET surface area means more exposed active sites, guaranteeing a higher activity. The normalized j_0 value observed for MoS₂/AC is larger than the commercial MoS₂ and annealed MoS₂.



Element	Weight	Atomic [%]
	[%]	
C	62.45	83.46
Mo	19.55	3.27
S	9.53	4.77
O	8.46	8.48
Total	100	100

Fig. S7 Element composition of the MoS₂/AC.

The EDS detection confirmed that the atomic ratio of Mo:S is 1:1.5, which is close to the MoS₂ stoichiometry, indicating the product are MoS₂ in theory. The strong presence of C in the composites is clearly the contribution from carbon provided by the carbonization of glucose. Residual oxygen-containing functional groups on the amorphous carbon contribute to the amount of oxygen that was measured to be 8.46% in weight. The signal of Cu arises from the TEM grid which is made of copper. In the table, we list the relative proportion of four elements in form of both weight and atomic.

References

1. Kibsgaard, J.; Chen, Z.; Reinecke, B. N.; Jaramillo, T. F., *Nat. mater.*, 2012, **11**, 963.
2. Wang, T.; Liu, L.; Zhu, Z.; Papakonstantinou, P.; Hu, J.; Liu, H.; Li, M., *Energy Environ. Sci.*, 2013, **6**, 625-633.